A small-molecule lycorine derivative reveals Na^+/K^+-ATPase α3 as an anti-obesity target

Yunfu Zhou[1,6], Henan Zhang[1,6], Duozhi Chen[2,6], Zhangcheng Chen[1], Yongtao Li[1], Chenyang Tian[3], Cong Zhang[1], Cen Li[4], Boran Chang[1], Rong Zeng[4], Jinsong Li[1], Xiaomin Song[1],Yan Chen[5], Xiaojiang Hao[2*], and Lin Li[1,3,5*]

[1]State Key Laboratory of Molecular Biology, State Key Laboratory of Cell Biology, CAS Center for Excellence in Molecular Cell Science, Institute of Biochemistry and Cell Biology, Chinese Academy of Sciences, University of Chinese Academy of Sciences, Shanghai 200031, China

[2]State Key Laboratory of Phytochemistry and Plant Resources in West China, Kunming Institute of Botany, Chinese Academy of Sciences, Kunming 650204, China

[3]School of Life Science and Technology, ShanghaiTech University, Shanghai 201210, China

[4]CAS Key Laboratory of Systems Biology, CAS Center for Excellence in Molecular Cell Science, Institute of Biochemistry and Cell Biology, Chinese Academy of Sciences, Shanghai 200031, China

[5]CAS Key Laboratory of Nutrition Metabolism and Food Safety, Shanghai Institute of Nutrition and Health, Chinese Academy of Sciences, Shanghai 200031, China

*Correspondence: Lin Li (lli@sibs.ac.cn) and Xiaojiang Hao (E-mail: haoxj@mail.kib.ac.cn).

[6]These authors contributed equally to this work.

Abstract

Obesity poses a global public health challenge and there is a huge unmet medical need for effective and safe anti-obesity therapeutics. Here, we discovered a small-molecule lycorine derivative designated as HLY72 that could potently promote lipolysis and reduce body weight in mice. Further study revealed that Na^+/K^+-ATPase α3 is the target of HLY72, and the Na^+/K^+-ATPase inhibitor digitoxin, but not istaroxime which could not go through blood-brain barrier, exhibits similar activities of reducing food intake and promoting lipolysis as HLY72 does in mice. Consistent with these findings, in knockin mice with a digitoxin-binding mutation T807C in Na^+/K^+-ATPase α3, but not in α1 gene, both digitoxin and HLY72 lose their activities. Furthermore, either chemical inhibition by HLY72 or genetic inhibition by T807C mutation of Na^+/K^+-ATPase α3 could effectively protect mice from diet-induced obesity. Therefore, we uncovered a previously unknown function of Na^+/K^+-ATPase α3 in the regulation of lipolysis and energy balance; and revealed a potential treatment and prevention strategy for obesity by targeting Na^+/K^+-ATPase α3.

Keywords:

Obesity, Na^+/K^+-ATPase α3, cardiac glycosides (CGs), lipolysis, Hormone-sensitive lipase (HSL)

Control of excess body fat is one of the greatest healthcare challenges of our time. In 2013, more than 2 billion adults were overweight worldwide and 34.3% adults in China was overweight in 2019[1,2]. Obesity has been recognized as a significant risk factor for a variety of serious conditions such as type 2 diabetes, atherosclerosis, cardiovascular disease, hypertension and even cancer[3-5]. Despite of great efforts in developing anti-obesity agents, most weight-loss drugs failed mainly due to their serious adverse effects affecting tolerability and safety[6]. Current pharmacological treatment options to reduce weight remain limited and generally lack satisfactory efficacies[5]. There is an unmet medical need for new therapeutic agents and targets to counteract the obesity epidemic.

Na^+/K^+-ATPase is an ubiquitous membrane transport protein, and required for creation and maintenance of the Na^+ and K^+ gradients across the cell membrane, thereby influencing cell volume, absorption, secretion, excitability and body homeostasis[7]. Na^+/K^+-ATPase consists mainly of two subunits, α and β subunits. The α subunit is the catalytic unit and also the target for pharmacological intervention, while β subunit may play a regulatory role[8]. There are four α isoforms for human Na^+/K^+-ATPase. The heart Na^+/K^+-ATPase α2 has been targeted for treating heart diseases. Small-molecule cardiac glycosides (CGs), such as digoxin and digitoxin, are the most notable class of Na^+/K^+-ATPase inhibitors that have been used for centuries to treat congestive heart failure[9,10]. In addition to the channel activity, studies have revealed the role of Na^+/K^+-ATPase α1 as an oxidant signaling transducer, which modulates reactive oxygen species amplification through an interaction with sarcoma-related kinase[11,12]. Studies showed that a peptide targeting Na^+/K^+-ATPase α1-Src interaction could affect adiposity[13,14].

Compared to the α1 and α2 isoform, the α3 isoform, encoded by the *ATP1A3* gene, is expressed almost exclusively in neurons[8,10]. Previous studies have revealed that different mutations in the *ATP1A3* gene cause varied diseases, however the exact underlying mechanisms remain largely unknown[15,16]. In the current study, starting with a small-molecule compound HLY72 as a chemical probe, we discovered a previously unrecognized function of Na^+/K^+-ATPase α3 in regulating lipolysis and energy homeostasis, which makes Na^+/K^+-ATPase α3 a potential therapeutic target for obesity treatment and prevention.

RESULTS

Lycorine derivative HLY-72 exhibits anti-obesity activity

Previously, we identified a small-molecule lycorine derivative HLY78 as a Wnt agonist (**Fig. 1a**)[17]. When tested the possible effects of HLY78 using mouse models, we noticed a significant reduction in food intake within 6 hours of HLY78 treatment (**Fig. 1b**). HLY78 analogs, HLY72 and HLY103 (**Fig. 1c**), were previously prepared as negative controls without Wnt agonist activity[17]. As shown in **Fig. 1d & 1e**, HLY72, but not HLY103, suppressed food intake in a dose-dependent manner when given to mice intraperitoneally (i.p.). These results implied that HLY78 suppresses food intake in a mechanism that is independent of Wnt/β-catenin signaling. To exclude possible effects on Wnt signaling, we used HLY72 in the rest of the studies with HLY103 serving as a negative control. Diet-induced obese (DIO) mice were given HLY72 or DMSO for 3 weeks. Compared to DMSO, HLY72 decreased body weight by nearly 20% (**Fig. 1f**); meanwhile, HLY72 reduced body fat composition (**Fig. 1g**). Hormone-sensitive lipase (HSL) is the key enzymes catalyzing lipolysis in the white adipose tissue, and its activity (reflected by its phosphorylation) is thought to be under tight control by the sympathetic nerve fibers that innervate the adipose tissue[18,19]. Protein kinase A (PKA) functions upstream of p-HSL, and its activity is reflected by the protein level of the phosphorylated PKA substrate[19]. We found that HLY72 significantly increased phosohparyaltion of both HSL and PKA substrate (**Fig. 1h**). Furthermore, the increased phosphorylation of HSL could be blocked by Hexamethonium, a sympathetic ganglion blocker (**Fig. 1i & 1j**). This result suggests that the neural inputs to adipose tissue is important for HLY72 to regulate lipolysis. Consistent with these results, glycerol and free fatty acid (FFA) were also increased in white adipose tissue after HLY72 treatment (**Fig. 1k**). Together, these results indicate an activity of HLY72 in reducing food intake and increasing lipolysis.

Na^+/K^+-ATPase α3 is identified as a potential target for HLY72

Given the fact that brain is the center of food intake and energy homeostasis regulation[20], we performed mass spectrometry (MS) analysis for proteins pulled down by biotinylated HLY72 (Bio72) from mouse brain lysates (**Extended Data Fig. 1**). We firstly confirmed a similar activity of biotinylated HLY72 as HLY72 in decreasing food intake (**Extended Data Fig. 2a**). Our MS analysis yielded 13 candidates (**Supplementary Table 1**), among which Na^+/K^+-ATPase α3 attracted our attention

due to a reported effect of Na^+/K^+-ATPase, especially α1, on body weight[14,21,22]. In mammals, there are four α isoforms (α1-4) of Na^+/K^+-ATPase, which are differentially expressed and have distinct functions[8]. Compared to the α1 isoform which is ubiquitously expressed and may play a "housekeeping" role, the rest three α isoforms of Na^+/K^+-ATPase have a more specific tissue distribution: α2 mostly in skeletal muscle and heart; α3 in neurons; and α4 predominantly in testes[8,10]. Our gene expression analysis also showed that α3 is specifically distributed in the brain (**Extended Data Fig. 2b**).

To estimate the possible effect of HLY72 on Na^+/K^+-ATPase activity, we purified Na^+/K^+-ATPase composed of α3 and β1 subunits, and confirmed its activity by using the classic Na^+/K^+-ATPase inhibitor digitoxin (**Fig. 2a & Extended Data Fig. 2c**). HLY72, but not HLY103, inhibited Na^+/K^+-ATPase activity by ~40% at a concentration of 10 μM (**Fig. 2b**); and the half maximal inhibitory concentration (K_i) of HLY72 was 18.58 μM (**Fig. 2c**). If Na^+/K^+-ATPase α3 was the target responsible for HLY72 anti-obesity activity, we reasoned that other Na^+/K^+-ATPase inhibitors might also have similar effects on food intake as HLY72. To test this, in addition to digitoxin, we introduced another two Na^+/K^+-ATPase inhibitors, oleandrin and istaroxime, both of which also effectively inhibited Na^+/K^+-ATPase α3 activity (**Extended Data Fig. 2d & 2e**). Despite the fact that these three compounds showed similar inhibitory activity against Na^+/K^+-ATPase *in vitro*, only digitoxin and oleandrin, but not istaroxime, significantly decreased food intake (**Fig. 2d**). The phosphorylation of HSL was also robustly increased in epididymal fat in response to digitoxin treatment, but not to istaroxime (**Fig. 2e & 2f**); and administration of hexamethonium significantly decreased the digitoxin-stimulated phosphorylation of HSL (**Extended Data Fig. 2f & 2g**). Digitoxin and oleandrin are reported to be capable of going through blood-brain barrier, but there is no such information available for istaroxime[23,24]. If the brain-localized Na^+/K^+-ATPase α3 was responsible for the effects we observed above, it is reasonable to surmise that Na^+/K^+-ATPase inhibitors function as anti-obesity agents only when they can access to the brain. To test this, we examined the brain distribution of HLY72, digitoxin and istaroxime. As shown in **Figure 2g & Supplementary Table 2**, HLY72 and digitoxin, but not istaroxime, could be detected in the brain. This result supports that Na^+/K^+-ATPase α3 in the brain could be the target for HLY72/digitoxin in regulating food intake and lipolysis.

Based on the crystal structure of pig Na^+/K^+-ATPase α1 complexed with digoxin (Protein Data Bank 7DDI)[25,26], we predicted possible binding sites for HLY72 on Na^+/K^+-ATPase by using AutoDock Vina docking program[27]. Four possible binding cavities were identified on pig α1 subunit surface, all of which are conserved in mouse α1 and α3 (**Extended Data Fig. 2h**). Among these four sites, site 4 encompassing T807 and F793 is also the classic binding site for cardiac glycosides (CGs) including digitoxin[28,29]. We then generated corresponding mutants for these four sites on mouse α3 followed by Na^+/K^+-ATPase activity assay. Our results showed that mutations targeting site 4, especially T807C, significantly decreased Na^+/K^+-ATPase's sensitivity to HLY72 (**Extended Data Fig. 2i-k**), implying that HLY72 binds to the same site on Na^+/K^+-ATPase as digitoxin. Of note, mutations of site 1, 2 and 4 all decreased Na^+/K^+-ATPase's ATPase activity, with T807C resulting in a decrease of ~50% (**Extended Data Fig. 2l**). This result is consistent with previous reports that T807C decreases Na^+/K^+-ATPase's ATPase activity[30]. To investigate whether Na^+/K^+-ATPase α3 could be the bona fide endogenous target for HLY72/digitoxin, we tried to construct *ATP1A1* T804C, *ATP1A2* T801C and *ATP1A3* T807C point mutation knockin (KI) mice through zygote injection method[31]. We successfully generated *ATP1A1* T804C and *ATP1A3* T807C mice (**Extended Data Fig. 3a & 3b**), with *ATP1A2* T801C generation failed. The body fat of *ATP1A1* T804C mice decreased slightly, with no significant changes for the body weight and muscle proportion, as compared to the wild-type (WT) control mice (**Fig. 2h)**. By contrast, *ATP1A3* T807C mutation significantly reduced body weight and body fat, accompanied by an increase of muscle proportion (**Fig. 2i)**. Compare to control WT, both *ATP1A1* T804C and *ATP1A3* T807C mice showed no difference in food intake (**Extended Data Fig. 3c**). In addition to measuring the body fat by using magnetic resonance, we also took out the white tissue of mouse epididymis and weighed it directly, which was significantly reduced in *ATP1A3* T807C *vs* WT control mice **(Fig. 2j)**. When compared to WT control mice, *ATP1A1* T804C mice showed no changes of HSL phosphorylation in white adipose tissue; by contrast, the p-HSL levels for *ATP1A3* T807C mice increased significantly **(Fig. 2k & Extended Data Fig. 3d)**. Glycerol and free fatty acid were also increased in white adipose tissue of *ATP1A3* T807C mice (**Fig. 2l**), while serum levels of glycerol and free fatty acid were unchanged (**Fig. 2m**). Expression of lipid metabolism-related genes in epididymal fat of mice was then examined. One of the key genes, *FAS* that is involved in fatty acid

synthesis, was increased; and other genes involved in lipolysis including HSL, fat storage and white fat browning remained unchanged (**Extended Data Fig. 3e**).

Next, we examined effects of HLY72 and digitoxin on food intake in *ATP1A1* T804C and *ATP1A3* T807C mice. After injection of HLY72 or digitoxin into *ATP1A1* T804C mice, the food intake remained reduced as compared to WT mice; while neither HLY72 nor digitoxin could induce any apparent effects on food intake in *ATP1A3* T807C mice **(Fig. 2n & 2o)**. Moreover, digitoxin treatment increased p-HSL of white adipose tissue in *ATP1A1* T804C mice to a similar extent as that in WT mice **(Fig. 2p)**; by contrast, it could not further increase p-HSL in *ATP1A3* T807C mice **(Fig. 2q)**. Together, these data provide *in vivo* evidence that the Na^+/K^+-ATPase α3 is the bona fide target for the activity of HLY72/digitoxin in regulating food intake and lipolysis in mice.

HLY72 treatment protects mice from HFD-induced obesity

Based on the finding above that HLY72/digitoxin could promote lipolysis and reduce food intake by targeting Na^+/K^+-ATPase α3, it is reasonable to postulate that HLY72/digitoxin treatment could also be able to effectively protect mice from HFD-induced obesity. To investigate this possibility, we examined the effect of HLY72 and digitoxin on HFD-fed mice with a reduced dose of 10 mg/kg and 5 μg/kg once every two days for a total of one and half months (**Fig. 3a**). As shown in **Figure 3b**, HLY72 and digitoxin, especially HLY72, led to a significantly less gain of weight during HFD as compared to the vehicle control. Meanwhile, HLY72 decreased food intake slightly with digitoxin showing no effect on food intake, while both of them did not affect the water intake of mice (Extended data **Fig. 4a & 4b**). When compared to the DMSO control, HLY72 treatment resulted in a significant reduction of body fat composition accompanied by an increase of body lean percentage, with digitoxin exhibiting no apparent activities (**Fig. 3c & 3d**).

Metabolic parameters were also measured for three groups of HFD-fed mice, namely digitoxin, HLY72, and DMSO group. Compared to the DMSO control, EE, especially during the dark cycle, was significantly increased in both digitoxin- and HLY72-treated mice with physical activity unchanged in these two groups; while, RER values was significantly increased in HLY72-treated mice with a slight increase in digitoxin group (**Fig. 3e-g**). In addition, oxygen consumption (VO_2) was increased during the dark cycle in both digitoxin and HLY72 group (**Fig. 3h**). Next, we

performed a glucose tolerance test (GTT) for the three groups. Clearance of glucose from the circulation during GTT was significantly faster in both digitoxin- and HLY72-treated mice than that in the vehicle-treated mice (**Fig. 3i**). Furthermore, insulin sensitivity in both digitoxin- and HLY72-treated mice was also improved, which were analyzed by an insulin tolerance test (ITT) (**Fig. 3j**). Notably, HFD-induced hepatic steatosis was largely ameliorated in both digitoxin- and HLY72-treated mice (**Fig. 3k**). Together, these results indicate that inhibition of Na^+/K^+-ATPase α3 by small molecule HLY72 and digitoxin, especially HLY72, could effectively protect mice from HFD-induced obesity and related metabolic syndromes in mice.

***ATP1A3* T807C mice exhibits resistance to HFD-induced obesity**

Our findings above showed that chemical inhibition of Na^+/K^+-ATPase α3 by HLY72/digitoxin could effectively protect mice from HFD-induced obesity. Next, we set out to investigate whether genetic inhibition of Na^+/K^+-ATPase α3 could also have the similar effects. For this, we took advantage of the property of the α3 T807C mutation—decreasing Na^+/K^+-ATPase activity by ~50%, and investigated potential effects of such a genetic inhibition of Na^+/K^+-ATPase α3 on metabolic features and lipolysis of HFD-fed mice. *ATP1A3* WT and T807C KI mutant mice were maintained on 60 kcal% high-fat diet for 8 weeks, and *ATP1A3* T807C mice gained significantly less body weight during HFD as compared to their WT counterparts with no influence on food intake and water intake (**Fig. 4a, b** & **Extended Data Fig. 4c, d**). The α3 mutant mice also showed a decreased percentage of body fat, accompanied by an increased percentage of body muscle (**Fig. 4c & 4d)**. The white adipose tissue of the whole epididymis was significantly lighter in α3 mutant mice versus WT mice **(Fig. 4e & 4f).** Compared with WT mice, α3 mutant mice showed increased EE, RER, physical activity and VO_2 (**Fig. 4g-j)**. Moreover, glucose homeostasis was improved and clearance of glucose from the circulation during GTT was significantly elevated in α3 mutant mice compared to the WT control mice **(Fig. 4k).** Insulin sensitivity was also improved as reflected by ITT **(Fig. 4l).** Notably, HFD-induced liver steatosis was largely ameliorated in α3 mutant mice when compared with WT control mice **(Fig. 4m).** Based on these results, we proposed that a decrease of Na^+/K^+-ATPase α3 activity facilitates lipolysis on one hand, and increases energy utilization on the other hand in mice, which together result in an efficient protection for *ATP1A3* T807C mice from die-induced obesity and related abnormities (**Fig 4n)**.

Discussion

Our studies here revealed that Na^+/K^+-ATPase inhibitors with access to brain could be potential agents for counteracting obesity. Isoforms of Na^+/K^+-ATPase α subunits are highly homologous and we do not think HLY72/digitoxin have selectivity towards different α subunit isoforms, which therefore might cause side effects. However, we believe that their anti-obesity effects are a specific outcome from targeting Na/K-ATPase α3 as reflect by the result that KI mice with the digitoxin-binding mutation in α3 but not in α1 gene abrogated HLY72/digitoxin's activity (**Fig. 2n-q)**. As such, we provided genetic evidence for Na^+/K^+-ATPase α3 as the bona fide target for HLY72/digitoxin. In addition, our results showed that HLY72/digitoxin, especially HLY72, could also effectively protect mice from HFD-induced obesity and related syndromes (**Fig. 3b & Fig. 3i-k)**. In line with this, genetic inhibition of Na^+/K^+-ATPase α3 by T807C mutation showed similar effects of protecting mice from HFD-induced obesity and related metabolic problems such as hepatic steatosis, hyperglycemia and insulin resistance (**Fig. 4k-m)**. Treatment of established obesity is normally quite challenging, and preventive intervention is an important alternative strategy to combat the obesity epidemic. Our findings here suggest that both chemical and genetic inhibition of Na^+/K^+-ATPase α3 exhibit robust protection against HFD-induced adiposity and related adverse effects in mice, thereby rendering Na^+/K^+-ATPase α3 a promising drug target not only for treatment but also for prevention of obesity.

Of note, HLY72 and digitoxin reduce food intake in both lean and obese mice; however, this phenotype was much weaker (HLY72) or disappeared (digitoxin) when these two compounds were administrated chronically with lower doses (**Extended Data Fig. 4a)**. Moreover, we also did not observe food intake reduction in *ATP1A3* T807C KI mice compared to WT control mice (**Extended Data Fig. 3c & Extended Data Fig. 4c)**. One possible reason is that there could be redundant satiation signaling pathways *in vivo* as depletion of some genes regulating food intake does not cause any phenotypes[32]. Therefore, a long period treatment of inhibitors or a genetic inhibition of Na^+/K^+-ATPase activity by α3 mutation may stimulate redundant signaling to compensate for the effect if Na^+/K^+-ATPase inhibition on food intake. Considering that the body weight remained decreased significantly in α3 mutation KI mice (**Fig. 2i & Fig. 4a, b)**, we tend to believe that a promotion of lipolysis and energy utilization,

rather than a reduction of food intake, could be the major mechanism behind the weight loss induced by Na^+/K^+-ATPase α3 inhibition.

Surprisingly, we found that HLY72 performs better in protecting mice from HFD-induced obesity than digitoxin does (**Fig. 3b & 3e-h**). This apparent paradox may attribute to a much shorter half-life of HLY72 (< 1 hour) than digitoxin (> 24 hours) *in vivo* as measured by the pharmacokinetic analysis (**Fig. 2g)**. As mentioned above, HLY72/digitoxin may cause side effects due to binding to other Na^+/K^+-ATPase α isoforms, such as binding to α2 to affect myocardial function. Therefore, a shorter half-life for anti-obesity agents like HLY72 may be beneficial to the host in regarding to reducing potential side effects. Moreover, Na^+/K^+-ATPase inhibitors with more specify towards α3 isoform and an access to brain could also be desired for anti-obesity purpose.

Inhibitors of Na^+/K^+-ATPase such as CGs have been used for centuries to treat congestive heart failure. In addition to CGs synthesized or isolated from plants, mammals including human also produce endogenous cardiac glycosides, mostly in blood, adrenal gland, and hypothalamus, which act as natural regulators of Na^+/K^+-ATPase[33]. However, our understanding of these endogenous cardiac glycosides is still quite incomplete. Our finding here that digitoxin can regulate lipolysis and body weight imply that the *in vivo* regulation of Na^+/K^+-ATPase by endogenous cardiac glycosides, if occur, may play a role in physiological energy homeostasis maintenance.

In summary, we discovered Na^+/K^+-ATPase α3 as a promising target for obesity prevention and treatment. However, the mechanism of Na^+/K^+-ATPase α3 regulating lipolysis and energy homeostasis remains unknown and warrants further exploration.

REFERENCES

1 Ng, M. *et al.* Global, regional, and national prevalence of overweight and obesity in children and adults during 1980-2013: a systematic analysis for the Global Burden of Disease Study 2013. *Lancet* **384** 766-781 (2014).

2 Pan, X. F., Wang, L. M. & Pan, A. Epidemiology and determinants of obesity in China. *Lancet Diabetes Endo* **9** 373-392 (2021).

3 Bray, G. A., Fruhbeck, G., Ryan, D. H. & Wilding, J. P. Management of obesity. *Lancet* **387** 1947-1956 (2016).

4 Saltiel, A. R. New therapeutic approaches for the treatment of obesity. *Sci Transl Med* **8** 323rv322 (2016).

5 Muller, T. D., Bluher, M., Tschop, M. H. & DiMarchi, R. D. Anti-obesity drug discovery: advances and challenges. *Nat Rev Drug Discov* **21** 201-223 (2022).

6 Krentz, A. J., Fujioka, K. & Hompesch, M. Evolution of pharmacological obesity treatments: focus on adverse side-effect profiles. *Diabetes Obes Metab* **18** 558-570 (2016).

7 Blanco, G. & Mercer, R. W. Isozymes of the Na-K-ATPase: heterogeneity in structure, diversity in function. *Am J Physiol-Renal* **275** F633-F650 (1998).

8 Matchkov, V. V. & Krivoi, II. Specialized Functional Diversity and Interactions of the Na,K-ATPase. *Front Physiol* **7** 179 (2016).

9 Prassas, I. & Diamandis, E. P. Novel therapeutic applications of cardiac glycosides. *Nat Rev Drug Discov* **7** 926-935 (2008).

10 Wang, H. Y. & O'Doherty, G. A. Modulators of Na/K-ATPase: a patent review. *Expert Opin Ther Pat* **22** 587-605 (2012).

11 Cui, X. Y. & Xie, Z. J. Protein Interaction and Na/K-ATPase-Mediated Signal Transduction. *Molecules* **22** (2017).

12 Liu, J., Lilly, M. N. & Shapiro, J. I. Targeting Na/K-ATPase Signaling: A New Approach to Control Oxidative Stress. *Curr Pharm Des* **24** 359-364 (2018).

13 Kutz, L. C. *et al.* The Na/K-ATPase alpha 1/Src interaction regulates metabolic reserve and Western diet intolerance. *Acta Physiol* **232** (2021).

14 Sodhi, K. *et al.* pNaKtide inhibits Na/K-ATPase reactive oxygen species amplification and attenuates adipogenesis. *Sci Adv* **1** e1500781 (2015).

15 Heinzen, E. L. *et al.* Distinct neurological disorders with ATP1A3 mutations. *Lancet Neurol* **13** 503-514 (2014).

16 Salles, P. A., Mata, I. F., Brunger, T., Lal, D. & Fernandez, H. H. ATP1A3-Related Disorders: An Ever-Expanding Clinical Spectrum. *Front Neurol* **12** (2021).

17 Wang, S. *et al.* Small-molecule modulation of Wnt signaling via modulating the Axin-LRP5/6 interaction. *Nat Chem Biol* **9** 579-585 (2013).

18 Zeng, W. *et al.* Sympathetic neuro-adipose connections mediate leptin-driven lipolysis. *Cell* **163** 84-94 (2015).

19 Recazens, E., Mouisel, E. & Langin, D. Hormone-sensitive lipase: sixty years later. *Prog Lipid Res*

82 (2021).

20 Rossi, M. A. & Stuber, G. D. Overlapping Brain Circuits for Homeostatic and Hedonic Feeding. *Cell Metabolism* **27** 42-56 (2018).

21 Iannello, S., Milazzo, P. & Belfiore, F. Animal and human tissue Na,K-ATPase in obesity and diabetes: A new proposed enzyme regulation. *Am J Med Sci* **333** 1-9 (2007).

22 Kurita, H. *et al.* Arcuate Na+,K+-ATPase senses systemic energy states and regulates feeding behavior through glucose-inhibited neurons. *Am J Physiol Endocrinol Metab* **309** E320-333 (2015).

23 Storstein, L., Nore, A. K. & Sjaastad, O. Studies on digitalis. 23. Blood-brain barrier of digitoxin in humans. *Clin Cardiol* **2** 146-150 (1979).

24 Ni, D. *et al.* Murine pharmacokinetics and metabolism of oleandrin, a cytotoxic component of Nerium oleander. *J Exp Ther Oncol* **2** 278-285 (2002).

25 Laursen, M., Gregersen, J. L., Yatime, L., Nissen, P. & Fedosova, N. U. Structures and characterization of digoxin- and bufalin-bound Na+, K+-ATPase compared with the ouabain-bound complex. *P Natl Acad Sci USA* **112** 1755-1760 (2015).

26 Laursen, M., Yatime, L., Nissen, P. & Fedosova, N. U. Crystal structure of the high-affinity Na+,K+-ATPase-ouabain complex with Mg2+ bound in the cation binding site. *P Natl Acad Sci USA* **110** 10958-10963 (2013).

27 Morris, G. M. *et al.* AutoDock4 and AutoDockTools4: Automated Docking with Selective Receptor Flexibility. *J Comput Chem* **30** 2785-2791 (2009).

28 Feng, J. N. & Lingrel, J. B. Analysis of Amino-Acid-Residues in the H5-H6 Transmembrane and Extracellular Domains of Na,K-Atpase Alpha-Subunit Identifies Threonine-797 as a Determinant of Ouabain Sensitivity. *Biochemistry-Us* **33** 4218-4224 (1994).

29 Qiu, L. Y., Koenderink, J. B., Swarts, H. G. P., Willems, P. H. G. M. & De Pont, J. J. H. H. M. Phe(783), Thr(797), and Asp(804) in transmembrane hairpin M5-M6 of Na+,K+-ATPase play a key role in ouabain binding. *Journal of Biological Chemistry* **278** 47240-47244 (2003).

30 Burns, E. L. & Price, E. M. Random Mutagenesis of the Sheep Na,K-Atpase-Alpha-1 Subunit Generates a Novel T797n Mutation That Results in a Ouabain-Resistant Enzyme. *Journal of Biological Chemistry* **268** 25632-25635 (1993).

31 Wang, H. Y. *et al.* One-Step Generation of Mice Carrying Mutations in Multiple Genes by CRISPR/Cas-Mediated Genome Engineering. *Cell* **153** 910-918 (2013).

32 Begg, D. P. & Woods, S. C. The endocrinology of food intake. *Nature Reviews Endocrinology* **9** 584-597 (2013).

33 Bagrov, A. Y., Shapiro, J. I. & Fedorova, O. V. Endogenous cardiotonic steroids: physiology, pharmacology, and novel therapeutic targets. *Pharmacol Rev* **61** 9-38 (2009).

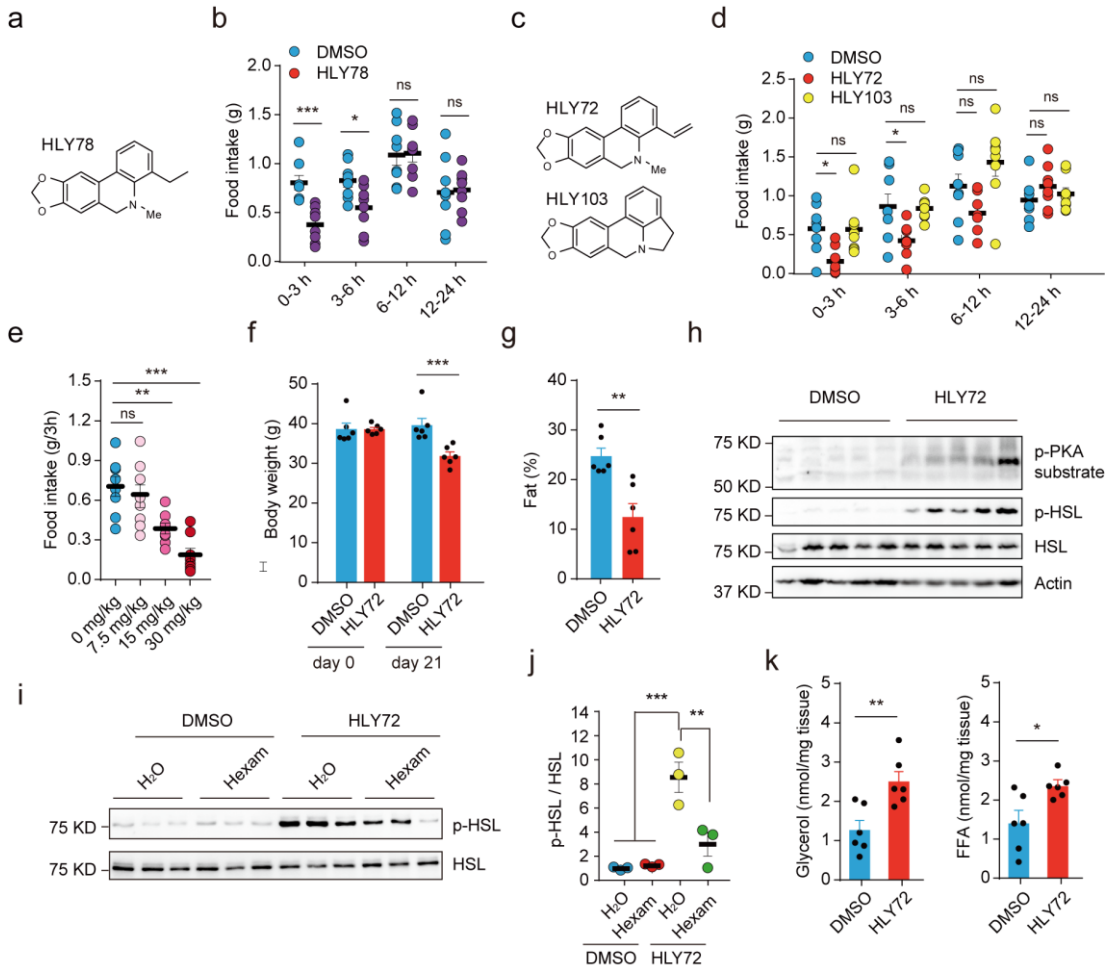

Figure 1. HLY72 reduces food intake and promotes lipolysis. a, Chemical structure of HLY78. **b**, Food intake after injection of HLY78 (20 mg/kg) or DMSO (n = 8 per group). **c**, Chemical structure of HLY72 and HLY103. **d**, Food intake after injection of HLY72 (20 mg/kg), HLY103 (20 mg/kg) or DMSO (n = 8 per group). **e**, Dose-dependent effect of HLY72 on food intake of mice (n = 8 per group). **f-g**, Mice were fed with 45 kcal% high-fat diet for 16 weeks and then subjected to three-day treatment (i.p.) regiments separated by 4 days non-treatment intervals of HLY72 (20 mg/kg) for 3 weeks of treatment (n = 6 per group). Representative figure for the changes of body weight (**f**) and fat mass proportion (**g**). **h**, Mice were peripherally administrated with HLY72 (20 mg/kg) for 6 hours, p-PKA-substrate and p-HSL in total protein extracts of epididymal fats were examined by immunoblot analysis (n = 5 per group). **i-j**, Mice were peripherally administrated with HLY72 (20 mg/kg) in combination with 40 mg/kg ganglionic blocker hexamethonium twice a day for 2 consecutive days. The sample was collected 6 hours after the second injection. p-HSL in total protein extracts of epididymal fats were examined by immunoblot

analysis (**i**), and analyzed statistically (**j**) (n = 3 per group). **k**, White adipose tissue glycerol and free fatty acid after two days of HLY72 (20 mg/kg per day) treatment. The sample was collected 6 hours after the second injection. All values are presented as mean ± s.e.m. *p* values were determined by two-tailed un-paired student's test in **b**, **g** and **k**, one-way ANOVA in **d**, **e**, **j** and two-way ANOVA in **f**. *****$p<0.05$, ******$p<0.01$, *******$p<0.001$ compared to control. ns, not significant.

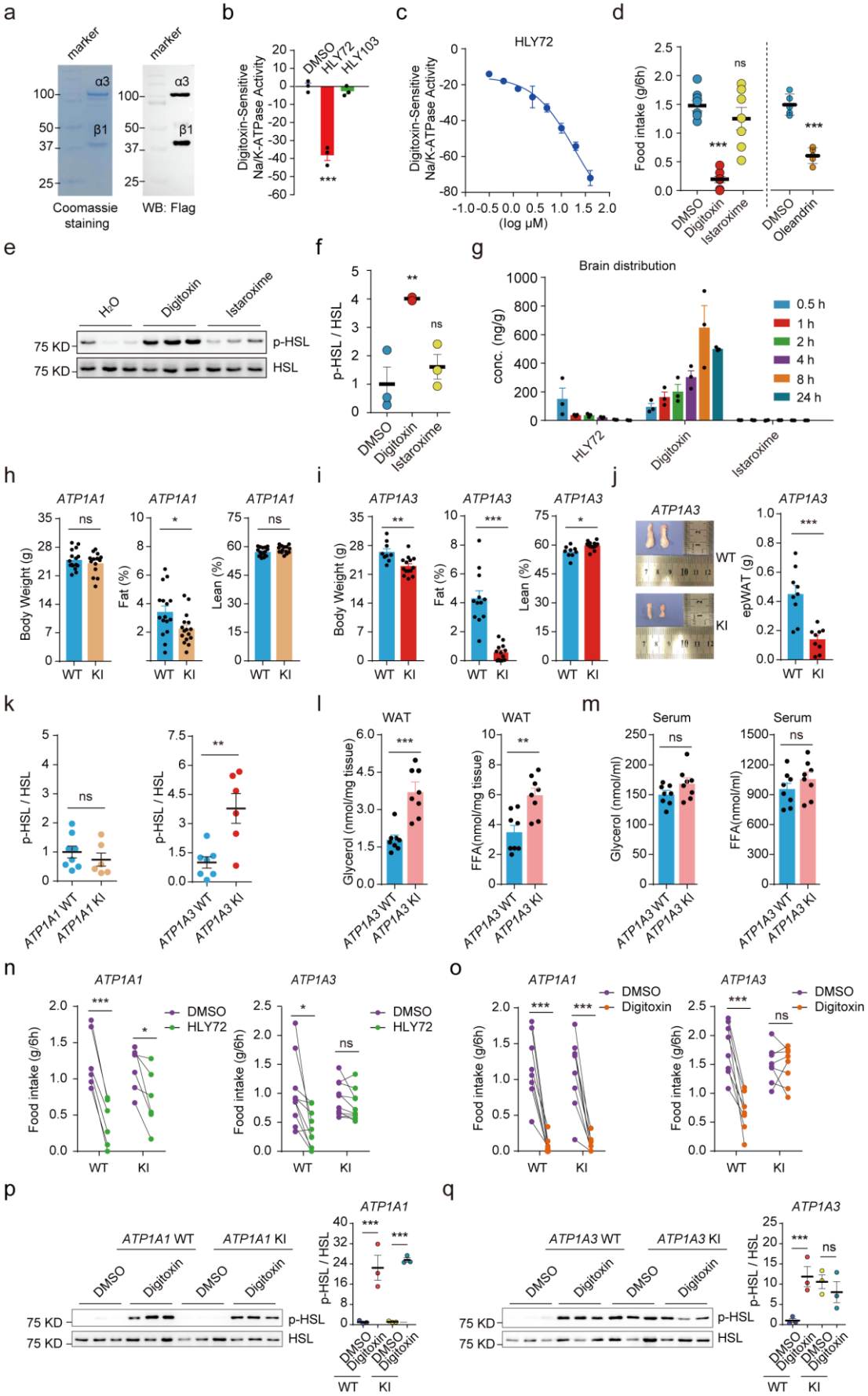
a
marker
α3
β1
100
50
37
25
Coomassie staining
WB: Flag
b
Digitoxin-Sensitive Na/K-ATPase Activity
DMSO
HLY72
HLY103
***
c
HLY72
Digitoxin-Sensitive Na/K-ATPase Activity
(log μM)
d
Food intake (g/6h)
ns
***
DMSO
Digitoxin
Istaroxime
Oleandrin
e
H2O
Digitoxin
Istaroxime
75 KD
p-HSL
HSL
f
p-HSL / HSL
**
ns
g
Brain distribution
conc. (ng/g)
0.5 h
1 h
2 h
4 h
8 h
24 h
HLY72
Digitoxin
Istaroxime
h
ATP1A1
Body Weight (g)
Fat (%)
Lean (%)
WT
KI
i
ATP1A3
j
epWAT (g)
k
p-HSL / HSL
ATP1A1 WT
ATP1A1 KI
ATP1A3 WT
ATP1A3 KI
l
WAT
Glycerol (nmol/mg tissue)
FFA(nmol/mg tissue)
m
Serum
Glycerol (nmol/ml)
FFA(nmol/ml)
n
Food intake (g/6h)
DMSO
HLY72
o
Digitoxin
p
q

Figure 2. HLY72 targets the Na^+/K^+-ATPase α3. a, Purified proteins of the mouse Na^+/K^+-ATPase α3β1. **b**, The effect of HLY72 (10 μM) and HLY103 (10 μM) on Na^+/K^+-ATPase α3β1 activity. **c**, Dose-dependent inhibition of Na^+/K^+-ATPase α3β1 activity by HLY72. **d**, Effects of digitoxin (200 μg/kg, i.p.), oleandrin (200 μg/kg, i.p.) and istaroxime (200 μg/kg, i.p.) on food intake of mice (n = 7 or 5 for DMSO group, n = 7 for digitoxin, istaroxime group, and n = 5 for oleandrin group). **e-f**, Mice were peripherally administrated with digitoxin (150 μg/kg), istaroxime (150 μg/kg) twice a day for 2 consecutive days. The sample was collected 6 hours after the second injection. p-HSL in total protein extracts of epididymal fats was examined by immunoblot analysis (**e**) and statistically analyzed (**f**) (n = 3 per group). **g**, Brain distribution of HLY72, digitoxin and istaroxime at different time points as indicated after oral administration (n = 3 per time point per group). **h-i**, The body weight, body fat (%) and muscle proportion of WT, *ATP1A1* T804C and *ATP1A3* T807C mice (8-week-old) (n = 16 for *ATP1A1* WT, n = 14-16 for *ATP1A1* T804C, n = 8-9 *ATP1A3* WT, n = 13-14 for *ATP1A3* T807C). **j**, Representative figures of the white adipose tissue of mouse epididymis in *ATP1A3* T807C and WT control mice (n = 9 per group). **k**, The p-HSL levels in white adipose tissue of *ATP1A3* T807C mice and *ATP1A1* T804C mice (n = 7 for *ATP1A1* WT and *ATP1A1* T804C, n= 7 for *ATP1A3* WT, n = 6 for *ATP1A3* T807C). For immunoblot analysis data, see Extended Data Figure 3d. **l-m**, Glycerol and free fatty acid levels in white adipose tissue and serum of *ATP1A3* T807C and WT control mice (n = 8 per group). **n-o**, Effects of HLY72 and digitoxin on food intake of WT, *ATP1A1* T804C and *ATP1A3* T807C mice (n = 6 or 10 for HLY72 treatment to *ATP1A1* and *ATP1A3* respectively, n = 8 for digitoxin treatment each group). **p-q**, Effects of digitoxin on p-HSL of white adipose tissue in *ATP1A1* T804C or *ATP1A3* T807C mice (n = 3 per group). Data are mean ± s.e.m. *p* values were determined by two-tailed un-paired student's test in **d** (right), **h-m,** two-tailed paired student's test in **n**, **o**, one-way ANOVA in **b**, **d** (left), **f**, **p** and **q**. ***$p<0.05$, ****$p<0.01$, *****$p<0.001$ compared to control. ns, not significant.

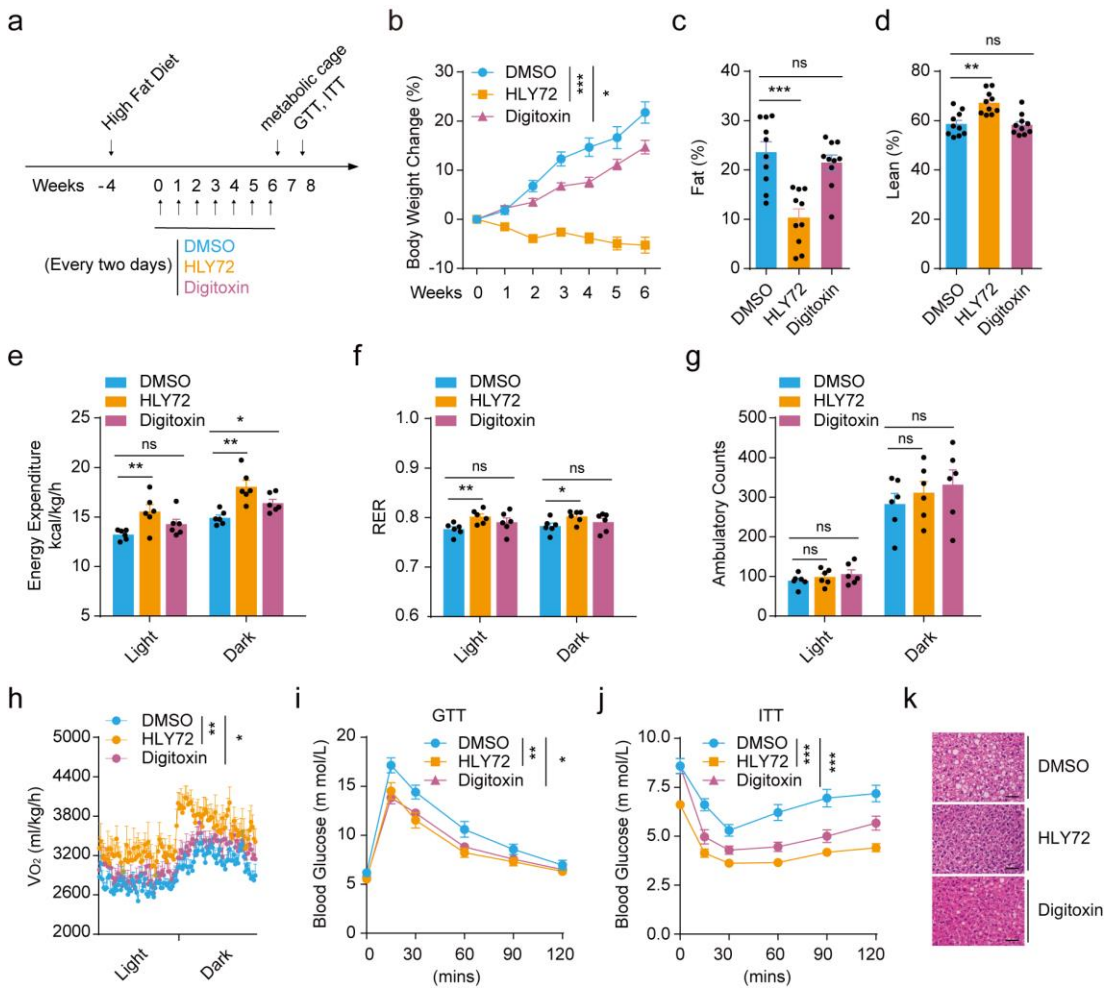

Figure 3. HLY72 or digitoxin treatment efficiently prevents mice from HFD-induced obesity. a, Schematic diagram of experiment study design. Mice (6-week-old) kept on 60 kcal% HFD were subjected by i.p. to digitoxin (5 μg/kg) or HLY72 (10 mg/kg) once two days for 6 weeks (n = 10 for each group). **b**, Body weight change of each group as descried in panel **a**. **c-d,** Effects of the HLY72/digitoxin treatment on the body fat composition (**c**) and percentage body lean (**d**) of mice. **e-h**, Effects of HLY72 and digitoxin on EE (**e**), RER (**f**), Activity (**g**) and VO_2 (**h**) were examined using 6 mice for each group of the above. **i-j**, Glucose tolerance test (GTT) and insulin tolerance test (ITT) results of HLY72 and digitoxin treatment (n = 9 for each group of above). One day before the two tests, mice were injected once with HLY72/digitoxin at the same doses as described in panel **a**. **k**, Hematoxylin and eosin staining of liver sections of HLY72- and digitoxin-treated mice (scale bar, 50 μm). Data are mean ± s.e.m. One-way ANOVA in **e-f** and two-way ANOVA in **b**, **g-l**. ***p*<0.05, ****p*<0.01, *****p*<0.001 compared to control. ns, not significant.

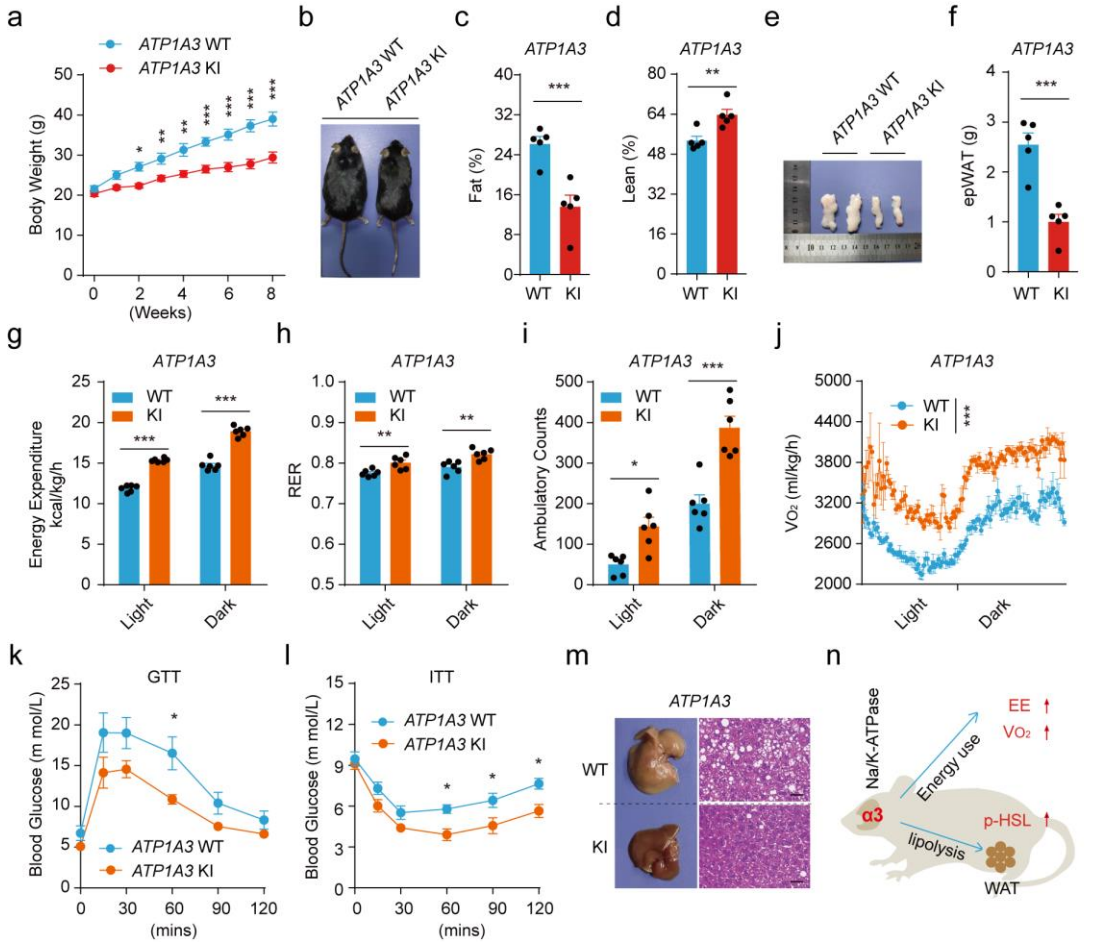

Figure 4. T807C mutation KI mice exhibits resistance to obesity and improvement of HFD-induced abnormalities. 6-week-old *ATP1A3* WT and T807C mice were maintained on 60% kcal high-fat diet for 8 weeks (n = 5 for each group). **a**, Comparison of body weight increase between *ATP1A3* WT and T807C mice. **b**, Representative picture showing body size of *ATP1A3* WT and T807C mice after 8 weeks of high-fat diet. **c-f**, Comparison of fat mass proportion (**c**), lean mass proportion (**d**) and epididymal fat (**e**, **f**) between *ATP1A3* WT and *ATP1A3* T807C mice. **g-j**, Individually caged *ATP1A3* WT and *ATP1A3* T807C mice were placed in metabolic cages, and EE (**g**), RER (**h**), physical activity (**i**) and VO_2 (**j**) were examined. Bar graphs represent average of two dark (24-36 hours and 48-60 hours) and two light (12-24 hours and 36-48 hours) cycles (n = 6 for each group). **k-l**, glucose tolerance test (GTT) and insulin tolerance test (ITT) results of *ATP1A3* WT and T807C mice (n = 5 for each group). **m**, Hematoxylin and eosin staining of liver sections (scale bar, 50 μm). **n**, A proposed model for Na^+/K^+-ATPase α3 function in body weight regulation. Data are mean ± s.e.m. Two-tailed student's test in **c**,**d**,**f** and

two-way ANOVA in **a**, **g-l**. ***p<0.05, ****p<0.01, *****p<0.001 compared to control. ns, not significant.

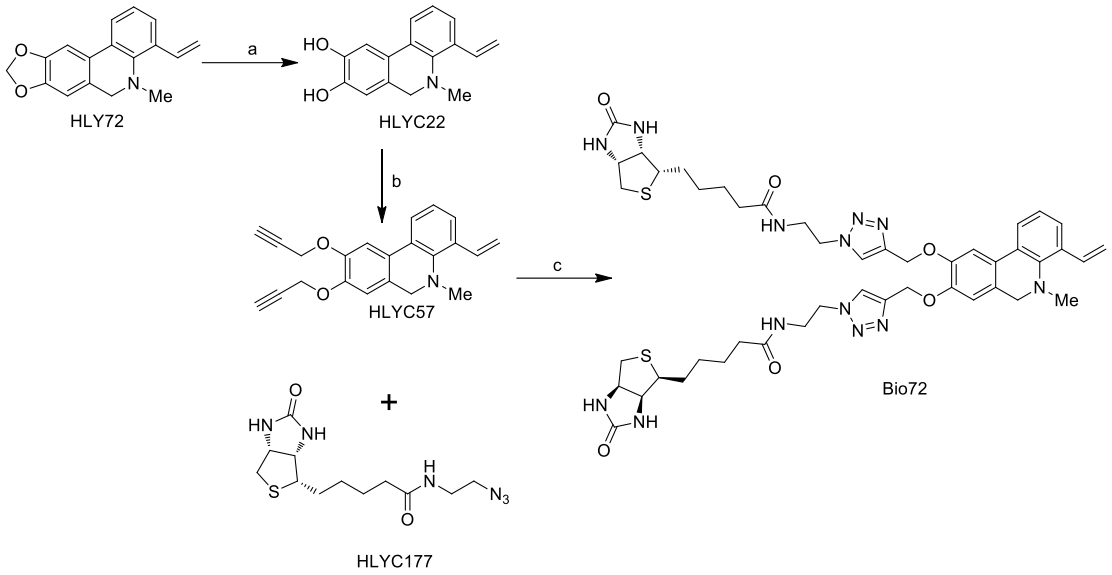

Extended Data Figure 1. The syntheses of biotinylated HLY72 (Bio72). Reagents and Conditions. **a**, Br_3B, CH_2Cl_2, -78°C, 6 hours, 70% for HLY119, 40% for HLYC22; **b**, Propargyl bromide, K_2CO_3, acetone, 75%; **c**, HLYC177, Sodium ascorbate, $CuSO_4$, TBA, 50°C, 12 hours, 50% for Bio72.

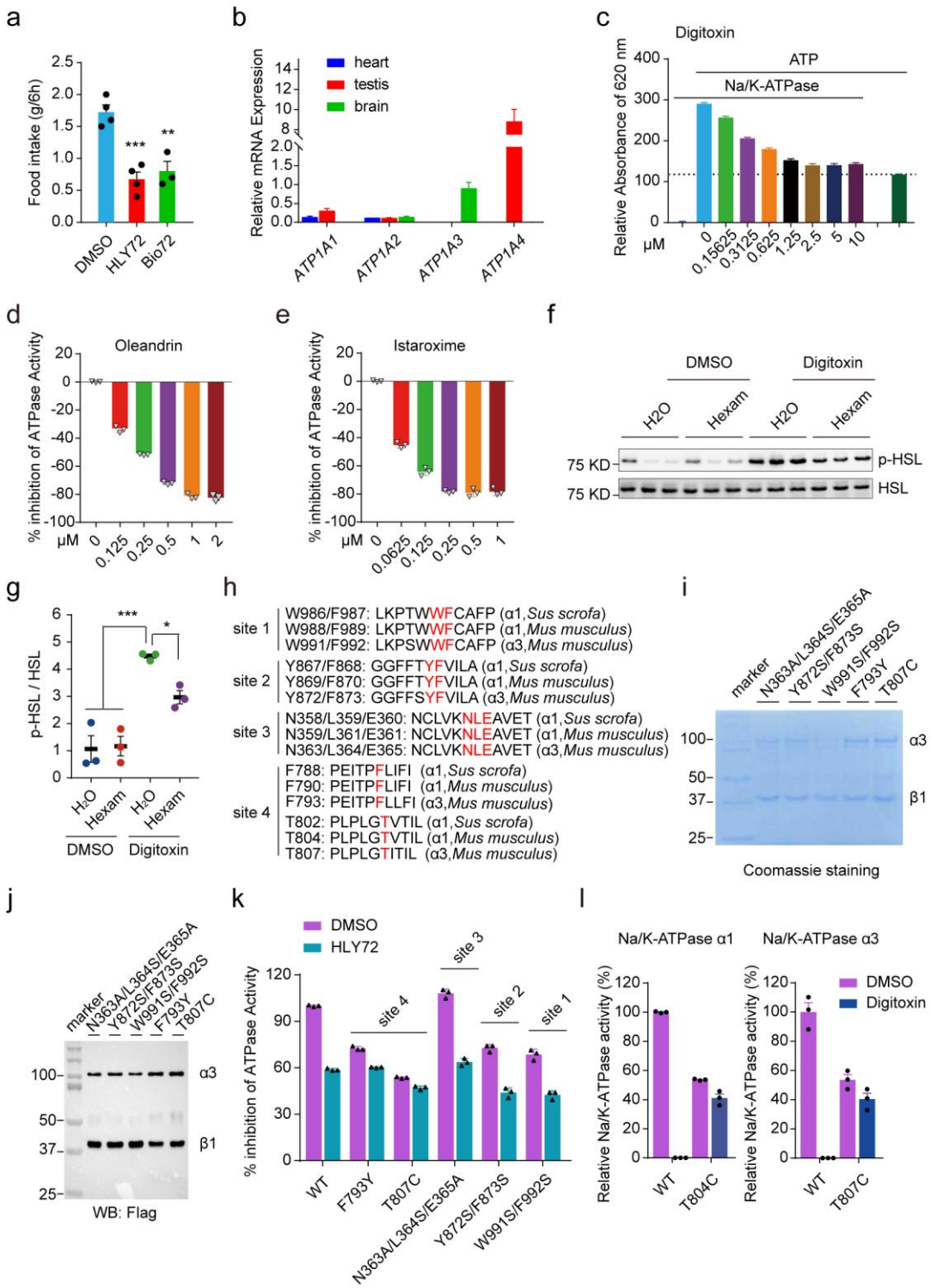

Extended Data Figure 2. Identification of Na^+/K^+-ATPase α3 as the target of HLY72. a, Bio72 (20 mg/kg) decreased food intake of mice as similar as HLY72 (20 mg/kg) (n = 3-4 per group). **b**, Expression of Na^+/K^+-ATPase α1-4 in different tissues as indicated. **c**, Evaluation of ATPase activity of the purified Na^+/K^+-ATPase α3β1 protein by using digitoxin. **d-e**, Evaluation of the inhibitory activity of oleandrin and istaroxime against the purified Na^+/K^+-ATPase α3β1. **f-g**, Mice (n = 3 per group) were

peripherally administrated with 150 μg/kg digitoxin in combination with 40 mg/kg ganglionic blocker hexamethonium twice a day for 2 consecutive days. The sample was collected 6 hours after the second injection. p-HSL in total protein extracts of epididymal fats was examined by immunoblot analysis (**f**) and statistical analysis (**g**). **h**, Comparison of amino acid sequences of pig Na^+/K^+-ATPase α1 with mouse Na^+/K^+-ATPase α1 and α3. **i-j**, Purification of mouse Na^+/K^+-ATPase comprising β1 and α3 WT or various α3 mutants designed according to docking results. **k**, Evaluation of α3 mutants for their sensitivities to HLY72. **l**, Effects of *ATP1A1* T804C or *ATP1A3* T807C mutation on Na^+/K^+-ATPase's sensitivity to digitoxin. Data are mean ± s.e.m. One-way ANOVA in **a** and **g**. ***p<0.05, ****p<0.01, *****p<0.001 compared to control.

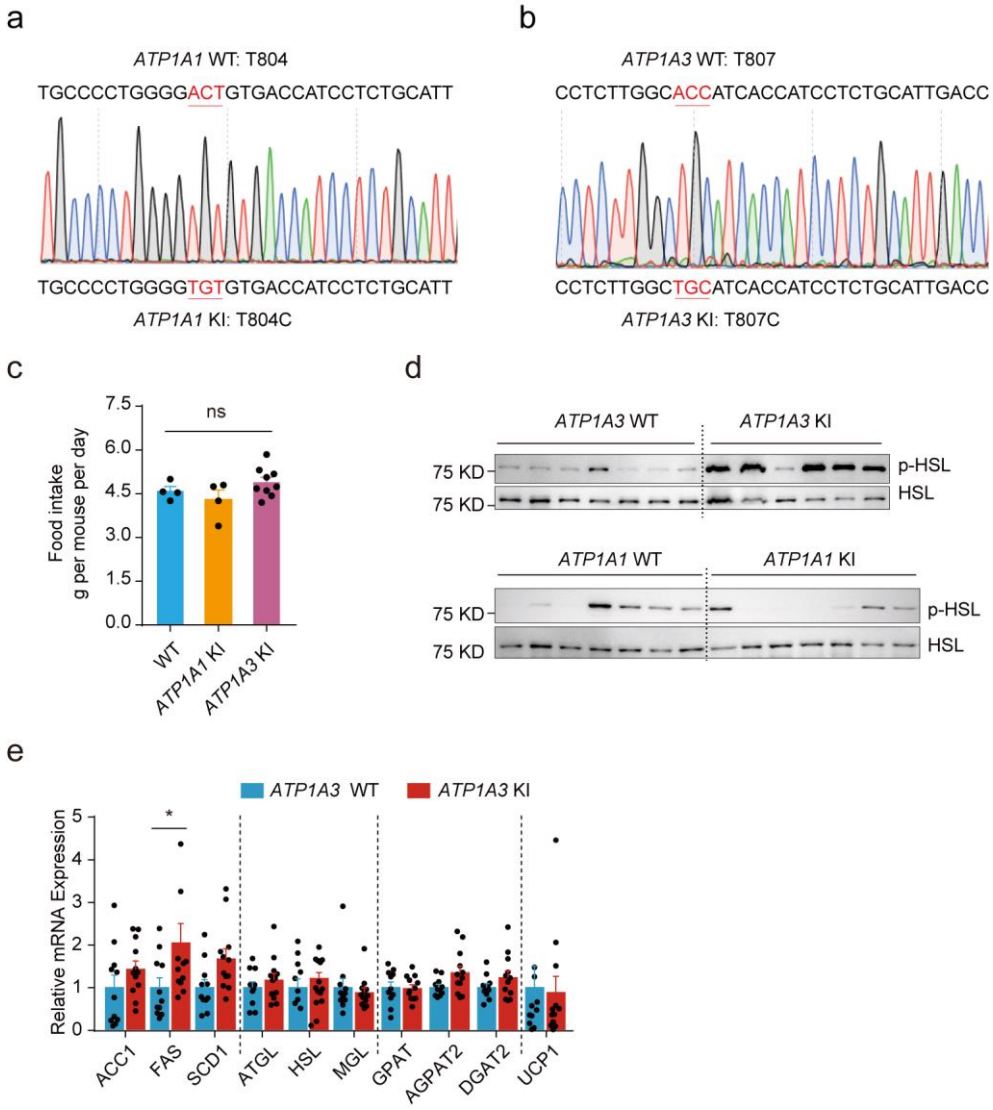

Extended Data Figure 3. Generation of *ATP1A1* T804C and *ATP1A3* T807C mice. **a**,**b**, Sequencing confirmed that *ATP1A1* T804C and *ATP1A3* T807C mutant mice were obtained. **c**, Average food intake of WT, *ATP1A1* T804C and *ATP1A3* T807C mutant mice (8-week-old) for two days (n = 4 for C57BL/6J as WT control and *ATP1A1* T804C, n = 9 for *ATP1A3* T807C). **d**, The p-HSL levels in white adipose tissue of *ATP1A3* T807C and *ATP1A1* T804C mice were examined. For statistical analysis, see Fig 2k. **e**, Expression of lipid metabolism-related genes in epididymal fat of *ATP1A3* WT and *ATP1A3* T807C mice. Data are mean ± s.e.m. Two-tailed student's test in **e** and one-way ANOVA in **c**. **p*<0.05, ***p*<0.01, ****p*<0.001 compared to control. ns, not significant.

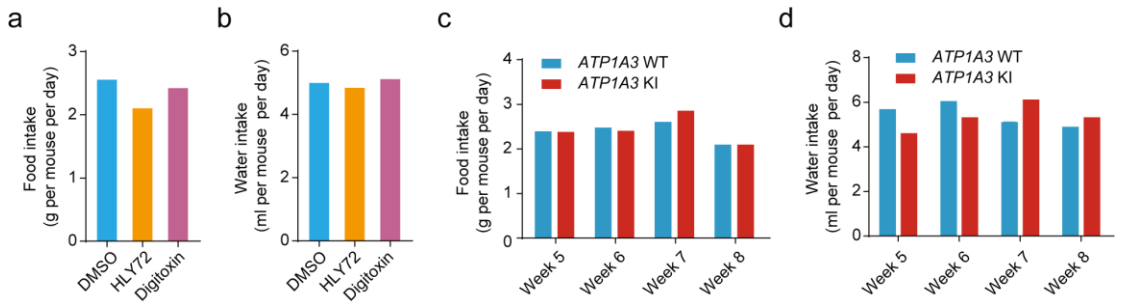

Extended Data Figure 4. Measurement of food and water intake. a-b, Data are present average food intake per mouse per day from week 1 to 4 (n = 10 per group) and average water intake per mouse per day from day 19 to 28 (n = 10 per group) as described in Fig. 3a. **c-d**, Average food intake (c) and water intake (d) of *ATP1A3* WT and *ATP1A3* T807C mice (n = 6 per group) every week during week 5-8 as described in **Fig. 4a**.

METHODS

Reagents and Plasmids. HSL antibody (#4107), Phospho-HSL (Ser-563) antibody (#4239) and p-PKA substrate anti-body (#9621) were purchased from Cell Signaling. HRP-conjugated anti-rabbit and anti-mouse antibodies were purchased from Thermo Scientific. ATPase/GTPase Activity Assay Kit was purchased from Sigma Aldrich (MAK113-1KT). Digitoxin (HY-B1357), Oleandrin (HY-13719), Istaroxime (HY-15718A), Captisol (HY-17031) and Hexamethonium Bromide (55-97-0) were purchased from MedChem Express. DDM (D100662) and DOPS (D130321) were obtained from Aladdin. Cholesterol (T0760) was obtained from TargetMol. $C_{12}E_8$ (P8925) was obtained from Sigma. TRIzol reagent was from Invitrogen. Dimethyl sulfoxide (DMSO) was from Calbiochem. *ATP1A1* (GenBank accession number NM_144900.2), *ATP1A3* (GenBank accession number NM_001290469.1) and *ATP1B1* (GenBank accession number NM_009721.6) were subcloned into pCMV vector to generate fusion protein with HA or Flag tag.

Chemical synthesis. HLY78, HLY72, HLY103, HLYC22, HLYC57, HLYC175-177 and HLY179 were synthesized by the procedures reported previously[1]. Chemical synthesis of the biotinylated HLY72 (Bio72) was as follows (**Extended data Fig. 1**): added HLYC57 (33.1 mg, 0.1 mmol) to HLYC177 (68.6 mg, 0.22 mmol) in H_2O/tBuOH (2 ml, 1:1), followed by the addition of $CuSO_4$ (1.8 mg) and sodium ascorbate solution (30 μl, 1 M solution). The reaction solution was stirred for 12 hours at 50°C. Then it was concentrated in vacuo, and the residue was purified by column chromatography with chloroform-methanol (9:1) to give Bio72 as a colorless solid.

Animals. Animal experiments were approved by The Animal Care and Use Committee at SIBCB. C57BL/6J mice were obtained from Animal Core Facility, SIBCB. For generation of diet-induced obese (DIO) mouse model, wild-type lean C57BL/6J male mice were placed on 45% or 60% kcal high fat diet (HFD; Research Diets) at the age of six weeks, and maintained on the same diet for 8-16 weeks before the experiments. Lean mice were kept on normal chow diet (NCD; 13.5% calories from fat) that was provided by Animal Core Facility, SIBCB. All mice were housed under 12 hours of light and 12 hours dark cycle, with the dark cycle encompassing 7 p.m. to 7 a.m., and they had free access to food and water unless otherwise described.

Food intake/body-weight measurements. The small molecules were administrated 2-3 hours before the dark cycle. For intraperitoneal (i.p.) experiment, mice were

acclimated for three days by daily intraperitoneal injection 25 μl of vehicle (DMSO) before small molecule treatment. Small molecules were dissolved in DMSO (25 μl) solution and injected into mice. Control group received 25 μl of DMSO during the course of experiment. Food intake and body weight were monitored as described in figure legend.

Mass spectrometry (MS). Total brain lysate was prepared and divided into two 1.5 ml EP tubes. HLY72 was added with a final concentration of 100 μM to one tube and equal volume of DMSO to another tube. The tubes were rotated at 4ºC for 30 min and centrifuged at 13,000 rpm for 10 min at 4ºC. Next, the supernatant was incubated with Streptavidin Agarose beads, which has been preincubated with 20 μM Bio72. After 2 hours of incubation, the beads were washed two times with lysis buffer and three times with PBS, and stored at -80ºC until MS analysis.

Na^+/K^+-ATPase α/β protein preparation. The Na^+/K^+-ATPase protein was prepared as described previously with modification[2]. The mouse *ATP1A1*, *ATP1A3* and *ATP1B1* expression vector (pCMV-Flag) were transfected to human HEK 293T cells. After 24-30 hours of transfection, cells were collected by centrifugation and the pellet was resuspended in buffer containing 1.4 M sorbitol, 10 mM Tris-HCl, pH 7.2, 1 mM EDTA, plus protease inhibitors (EDTA free). The sample was then lysed in a glass homogenizer proper strokes, followed by centrifugation at 10,000 g for 10 min at 4ºC. The supernatant was further centrifuged at 100,000 g for 1 hour. The precipitate was homogenized well with DDM (2:1 w/w) in a medium containing 20 mM Tris-HCl, pH 7.4, 250 mM NaCl, 0.1 M PMSF, and 10% glycerol. The insoluble material was removed by centrifugation at 12,000 g. The soluble material was incubated for 4 hours at 4ºC with anti-Flag M2 magnetic beads (Sigma). Beads was washed with buffer containing 20 mM Tris-HCl, pH 7.4, 100 mM NaCl, 0.1 mg/ml $C_{12}E_8$, 0.05 mg/ml DOPS, 0.01 mg/ml Cholesterol and 10% glycerol. The Na^+/K^+-ATPase α1/β1 and α3/β1 was eluted by mixing the beads with washing buffer containing flag peptide (DYKDDDDK, 500 μg/ml) 2 hours at 4ºC. The eluted protein was stored at -80ºC.

Assay of Na^+/K^+-ATPase activity. The ATPase/GTPase Activity Assay Kit was used to measure Na^+/K^+-ATPase activity, with modification as reported[3]. The ATP-hydrolyzing activity of Na^+/K^+-ATPase was defined as the digitoxin-sensitive hydrolysis of ATP in the presence of both Na^+ and K^+ with or without digitoxin (2.5

μM). Briefly, the incubation mixture containing samples in a final volume of 45 μl were prepared on ice. Firstly, small molecules or DMSO were added to the assay buffer (10 mM HEPES, pH 7.4, 130 mM NaCl, 20 mM KCl, 4 mM $MgCl_2$, 5% DMSO) in a volume of 15 μl. Next, Na^+/K^+-ATPase α1/β1 protein diluted in 15 μl assay buffer was added. Lastly, 3 mM of ATP in 15 μl assay buffer was added. The reaction was incubated for 30 min at 37°C and immediately put on ice to terminate the enzyme reaction. The free phosphate was then measured as described in the kit instruction manual. IC_{50} was calculated by Graphpad Prism 7.

Generation of *ATP1A1* T804C and *ATP1A3* T807C knockin mice via zygote injection. The T7 promoter sequence was fused with the Cas9 coding region which was cloned from pX260 plasmid (Addgene #42229). Similarly, T7 promoter sequence and the targeting sequence of *ATP1A1* and *ATP1A3* were fused to the guide RNA scaffold which was cloned from pX330 plasmid (Addgene # 42230). *In vitro* transcription of Cas9 mRNA and sgRNAs targeting *ATP1A1* and *ATP1A3* was performed with mMESSAGE mMACHINE T7 ULTRA Kit (ThermoFisher Scientific, AM1345, USA) and MEGAshortscript T7 Kit (ThermoFisher Scientific, AM1354, USA) according to the manufacturer's instructions, respectively. Both Cas9 mRNA and sgRNAs were then purified using MEGAclear Transcription Clean-Up Kit (ThermoFisher Scientific, AM1908, USA) and stored at -80°C. One-cell embryos were collected from superovulated wild-type C57BL/6J female mice that had been mated with wild-type C57BL/6J male mice. Cas9 mRNA (50 ng/μl), sgRNA targeting *ATP1A1* or *ATP1A3* (50 ng/μl) and donor (SSODN, 100 ng/μl) were mixed together and then injected into the one-cell embryos. The injected embryos were cultured in EmbryoMax KSOM Medium (Sigma-Aldrich, MR-106-D, USA) until the two-cell stage, followed by transferring into oviducts of recipients at 0.5 dpc. Recipient female mice delivered pups at 19.5 dpc. The first generation of point-mutant mouse were identified using the genotyping primers listed below. The mice harboring the correct point mutation were crossed for expansion of the mouse population.

In vitro transcription: *ATP1A1* sgRNA-F, TAATACGACTCACTATAGGGAG AGGATGGTCACAGTCCCCGTTTTAGAGCTAGAA; *ATP1A1* sgRNA-R, AAAA AAGCACCGACTCGGTG. *ATP1A3* sgRNA-F, TAATACGACTCACTATAGGGA GGATGGTGATGGTGCCAAGGTTTTAGAGCTAGAA; *ATP1A3* sgRNA-R, AAA AAAGCACCGACTCGGTG. Cas9 RNA F, TAATACGACTCACTATAGGGAGAT TTCAGGTTGGACCGGTG; Cas9 RNA R, GACGTCAGCGTTCGAATTGC. *AT*

P1A1-SSODN: ACCCCCTTCTTGATATTTATTATTGCAAACATTCCACTG CCC CTGGGGTGTGTGACCATCCTCTGCATTGACTTGGG CACTGACATGGTACGT GAGTGT. *ATP1A3*-SSODN: ACACCCTTCCTGCTCTTCATCATGGCTAACATC CCACTGCCTCTTGGCTGCATCACCATCCTCTGCATTGACCTGGGTACCGACA TGGTAAGCCTGGCT. Primers for genotyping: *ATP1A1* check-F, AGCACCTTT AAGAGGCCACC; *ATP1A1* check-R, ATGTTAAATGGGAGACCTGGCA. *ATP1 A3* check-F, CCATCGCCTACACTCTGACT; *ATP1A3* check-R, TGATGAGCCT TTCGTTGACCA.

RNA extraction, complementary DNA synthesis and quantitative real-time PCR. The tissues of mice were removed and total RNA was isolated with a TRIzol kit. Reverse transcription of purified RNA was performed using random hexamers primers and Superscript III reverse transcriptase according to the manufacturer's instructions (Invitrogen). Quantitative RT-PCR was performed with the TaKaRa SYBR Premix Ex Taq kit on the ABI-QuantStudio 6 Realtime PCR system.

The specific primers used for detecting the genes are as follows (forward primer first, reverse primer second, in 5′ - 3′ orientation)：*GPAT*, GGCCTTCG GATTATCCCTGG, CTTGGGGGCTCCTTTCTGAA; *AGPAT*, CAGCCAGGTTCT ACGCCAAG, TGATGCTCATGTTATCCACGGT; *DGAT*, ACTGGAACACGCCC AAGAAA, GTAGTCTCGGAAGTAGCGCC; *ACC1*, ATGGGCGGAATGGTCTC TTTC, TGGGGACCTTGTCTTCATCAT; *FAS*, GGAGGTGGTGATAGCCGGTAT, TGGGTAATCCATAGAGCCCAG; *SCD1*, CGAGGGCTTCCACAACTACC, AAC TCAGAAGCCCAAAGCTCA; *ATGL*, CAACGCCACTCACATCTACGG, GGAC ACCTCAATAATGTTGGCAC; *HSL*, GATTTACGCACGATGACACAGT, ACCT GCAAAGACATTAGACAGC; *MGL*, AGGCGAACTCCACAGAATGTT, ACAAA AGAGGTACTGTCCGTCT; *ACTB*, GCTGTATTCCCCTCCATCGTG, CACGGT TGGCCTTAGGGTTCA; *UCP1*, AGGCTTCCAGTACCATTAGGT, CTGAGTGA GGCAAAGCTGATTT. The relative expression of genes of interest was calculat ed by comparative CT method, and ACTB was used as endogenous controls.

Metabolic cage measurements. Animals were individually caged for at least three days before performing the metabolic chamber experiments. Columbus Instruments Comprehensive Lab Animal Monitoring System (CLAMS) was used for metabolic measurements in Animal Core Facility, SIBCB. Respiratory-exchange-ratio (RER), energy expenditure (EE), VO_2 and activity of mice were measured or calculated by

CLAMS. The first recorded cycle in the metabolic chambers was named as ″Dark 1 Cycle″. Dark 1 cycle was followed by Light 1, Dark 2, Light 2, Dark 3 and Light 3 cycles. We used data from Light 1+2 cycles and Dark 2+3 cycles of the experiments for analysis.

Glucose tolerance and insulin tolerance tests. For glucose tolerance tests, mice were fasted overnight and i.p. injected with glucose at 1 g/kg body weight. Blood glucose levels were measured at 0, 15, 30, 45, 60, 90 and 120 mins. For insulin tolerance tests, mice were fasted for 5 hours, and i.p. injected with 0.75 U/kg insulin. Blood glucose levels were measured at 0, 15, 30, 45, 60, 90 and 120 mins.

Body composition measurements. Total lean mass and fat percentage of mice were assessed using Bruker minispec LF50 mq7.5 NMR Analyzer in Animal Core Facility, SIBCB.

H&E staining. Mice liver tissue were dissected and stored in 4% paraformaldehyde phosphate buffer for one day. Liver were embedded in paraffin, sectioned, and stained with hematoxylin and eosin (H&E).

Lipolysis analysis and hexamethonium bromide treatment. To examine the effect of HLY72, digitoxin and istaroxime treatment on lipolysis, these molecules or DMSO were injected. After 5-6 hours, epididymal fat were collected and HSL phosphorylation was detected by western blotting. Hexamethonium bromide was injected 10 min after HLY72 and digitoxin administration. *ATP1A1* WT/T804C or *ATP1A3* WT/T807C mice were injected with HLY72 or digitoxin for 5-6 hours and epididymal fat tissues were then collected in the same way as described above. Glycerol and FFA were measured by Free Glycerol Assay Kit (ab65337) and Free Fatty Acid Assay Kit (ab65341).

Pharmacokinetics. The male ICR (CD-1) mice were used and acclimated for at least 1 week before the experiment. All the mice have been fasted for 12 hours before compound administration and remained under fasting for 2 hours. In tissue distribution investigation, mice were randomly assigned into six groups corresponding to the six collection time points (0.5, 1, 2, 4, 8 and 24 hours post administration) and seven groups in the rest pharmacokinetics study corresponding to the seven collection time points (0.25, 0.5, 1, 2, 4, 8 and 24 hours post administration). Blood samples were collected and centrifuged to obtain plasma samples. After washed with saline

and dried with filter paper, brain and heart tissues were then accurately weighed and homogenized in saline (5 ml/g tissue) on ice with an IKA T 10 basic homogenizer.

For determination of compounds in biological samples, a liquid chromatography-triple quadrupole mass spectrometry (LC-MS/MS) method was applied on Agilent 1200 RRLC tandem 6410 triple quadrupole mass spectrometers with an electrospray ionization source (ESI) (Agilent Technology, Santa Clara, CA, United States). Chromatographic separation was performed on an Agilent Poroshell 120 EC-C_{18} column (3.0 × 50 mm, 2.7 μm) tandem pre-column of Welch Analytical Guard Cartridges Ultimate XB-C_{18} (2.1 × 10 mm, 3 μm) at column temperature of 40°C. The mobile phase consists of 0.1% formic acid (*v/v*) in methanol (A) and 0.1% formic acid (*v/v*) aqueous solution (B). For plasma and tissue homogenate, the linear gradient elution program was: 0-1.6 min, 60-0% B; 1.6-2.0 min, 0% B; 2.0-2.1 min, 0-60% B; 2.1-4.0 min, 60% B. For urine and feces samples, to eliminate the severe matrix effect on excreta and determine other metabolites simultaneously, a different elution program was set as follows: 0-1.6 min, 80-0% B; 1.6-2.6 min, 0% B; 2.6-2.7 min, 0-80% B; 2.7-5.0 min, 80% B. The flow rate was 400 μl/min, and RRLC effluent was introduced directly to the mass spectrometer without splitting.

Mass spectrometry detector was operated in negative and multiple reaction monitoring (MRM) mode at unit mass resolution with a dwell time of 200 ms for all test compounds. The transitions and corresponding fragmentors, collision energies (CE) were optimized. The ion source parameters were Capillary 4000 V, Gas Flow 10 L/min, Nebulizer 25 psi, Gas Temperature 350°C for maximum sensitivity. Other MS parameters were adopted from the recommended values for the instrument.

Statistical analysis. Animals were grouped in a blinded and randomized way. All data were presented as means ± s.e.m or means ± sd as indicated. Statistical significance was measured via Student's t test (two-tailed) or one-way or two-way ANOVA, as indicated in the figure legends. Significance was accepted at ***P<0.05, ** P <0.01, *** P <0.001.

1 Wang, S. *et al.* Small-molecule modulation of Wnt signaling via modulating the Axin-LRP5/6 interaction. *Nat Chem Biol* **9** 579-585 (2013).

2 Jorgensen, P. L. Purification and characterization of (Na+ plus K+)-ATPase. IV. Estimation of the purity and of the molecular weight and polypeptide content per enzyme unit in preparations from the outer medulla of rabbit kidney. *Biochim Biophys Acta* **356** 53-67 (1974).

3 Strugatsky, D., Gottschalk, K. E., Goldshleger, R., Bibi, E. & Karlish, S. J. Expression of Na^+/K^+-ATPase in Pichia pastoris: analysis of wild type and D369N mutant proteins by Fe^{2+}-catalyzed oxidative cleavage and molecular modeling. *J Biol Chem* **278** 46064-46073 (2003).

ACKNOWLEDGEMENTS

We acknowledge Dianqing Wu at Yale School of Medicine for his constructive suggestions, and Wenwen Cai and Guoyuan Chen at SIBCB for their helps in mouse experiment, protein purification and metabolic chamber experiments. This work was supported by the National Natural Science Foundation of China (92053201) and CAS Strategic Priority Research Program (XDB19030000).

AUTHOR CONTRIBUTIONS

Y.Z. designed the study, performed or participated in most of the experiments, and prepared the manuscript. H.Z. performed most of the experiments about Na^+/K^+-ATPase KI mice. D.C. prepared all the HLY72-related compounds, and performed drug pharmacokinetic study. Z.C. contributed to HLY78 treatment experiments in mice. C.T., Y.L. and C.Z. assisted with GTT, ITT experiment, reagent preparation and mouse care. C.L. and R.Z. performed the mass spectrometry analyses. B.C. and J.L. generated Na^+/K^+-ATPase KI mice. X.S. assisted with protein expression and participated in manuscript preparation. Y.C. provided constructive suggestions about lipolysis related analysis. X.H. acquired funding, designed HLY72-related compounds, and assisted with project supervision. L.L. directed the project and designed the study of Na^+/K^+-ATPase KI mice, obtained financial support, and participated in manuscript preparation.